



WATEREYE

Project Title:	O&M tools integrating accurate structural health in offshore energy
Starting date:	2019/11/01
Duration in months:	36
Call (part) identifier:	H2020-LC-SC3-2019-RES-TwoStages
Grant agreement no:	851207

Consortium Members

Organisation	Abbreviation	Country
Centro Tecnológico Ceit-IK4	CEIT	Spain
Delft Dynamics B.V.	DD	The Netherlands
Semantic Web Company	SWC	Austria
Delft University of Technology	TUD	The Netherlands
SINTEF Energy Research AS	SINTEF-E	Norway
SINTEF AS	SINTEF-I	Norway
FLANDERS MAKE VZW	FMAKE	Belgium
COBRA Instalaciones y Servicios	COBRA	Spain
Plataforma Oceánica de Canarias	PLOCAN	Spain

Deliverable D4.2

Real-time probabilistic analysis of wind farms

Due date of deliverable	Month 30
Actual submission date	2022-09-30
Organisation name of lead contractor for this deliverable	SINTEF Energy Research
Dissemination level	Public
Revision	2.0

The WATEREYE project has received funding from the European Union's Horizon 2020 research and innovation programme under grant agreement No. 851207

Authors

Author(s)	Partner 5 (SINTEF-E) Valentin Chabaud, Konstanze Kölle
Contributor(s)	Partner 1 (CEIT) Ainhoa Cortes Vilda
	Partner 5 (SINTEF-E) Karl Merz, John Olav Tande

Disclaimer

The content reflects only the authors' view and the Agency is not responsible for any use that may be made of the information it contains.

DRAFT PREPARATION			
Version	Publication date	Content	Author
0.0	04/02/2022	<ul style="list-style-type: none"> ▪ First Draft 	<ul style="list-style-type: none"> ▪ Konstanze Kölle (SINTEF-E)
0.1	27/05/2022	<ul style="list-style-type: none"> ▪ Added content 	<ul style="list-style-type: none"> ▪ Valentin Chabaud, Konstanze Kölle (SINTEF-E)
1.0	26/09/2022	<ul style="list-style-type: none"> ▪ Added simulation results ▪ Discussion of results 	<ul style="list-style-type: none"> ▪ Valentin Chabaud, Konstanze Kölle (SINTEF-E)
1.1	28/09/2022	<ul style="list-style-type: none"> ▪ Incorporated review by CEIT 	<ul style="list-style-type: none"> ▪ Ainhoa Cortes Vilda (CEIT), SINTEF-E
2.0	30/09/2022	<ul style="list-style-type: none"> ▪ Completion 	<ul style="list-style-type: none"> ▪ Valentin Chabaud (SINTEF-E)

HISTORY OF CHANGES		
Version	Publication date	Change
0.0	04/0/2022	▪ First draft of the document
1.0	26/09/2022	▪ Final draft of the document
2.0	30/09/2022	▪ Final document

EXECUTIVE SUMMARY

The present document constitutes the report about the probabilistic analysis tool developed as part of the project titled “O&M tools integrating accurate structural health in offshore energy” (Project acronym: WATEREYE; Grant Agreement No. 851207).

The overall suggested approach for multidisciplinary probabilistic decision making is through the joint effect of fatigue- and corrosion-induced failures on O&M planning for offshore wind farms. The focus is set on the methodology of integrating aero-hydro servo analyses of wind *farms* (and not only their individual turbines) and subsequent fatigue damage calculations into medium-term decision making (weeks-ahead O&M planning), opening the way for combination with corrosion-related inspections or hypothetical repairs.

This deliverable starts with discussing the two methods that have been applied in WATEREYE to propagate stochastic dynamics in wind turbines. One method is using probabilistic state-space models for analyses in the frequency domain which was applied in WATEREYE Deliverable D4.1. The second method is to perform Monte-Carlo simulations in the time domain which is where the contributions of the present deliverable are.

A module that supports computationally efficient multiscale stochastic simulations of farm-scale turbulence has been developed. The module has been named TurbSim.Farm as it can be seen as an extension of NREL's TurbSim from turbine to farm scale. TurbSim.Farm provides coherent farm-scale turbulence by modelling an aggregated turbulent wind field between turbines for use in wake dynamics computations. It can be used as an add-on providing wind field as input to NREL's FAST.Farm. The main motivation is to capture power fluctuations to be used in multi-objective hierarchical wind farm control: tracking a power command from the grid instead of maximising power offers the possibility to derate selected turbines based on their fatigue damage index. This fatigue damage may in turn lead to failures to be handled by O&M planning together with corrosion-related failures, hence closing the loop with the rest of the WATEREYE project.

The concept of synthetic generation of farm-scale aggregated turbulence and its implementation in TurbSim.Farm has been verified and its efficiency proven. Compared with the state-of-the-art CFD-based solution, efficiency is drastically improved. Nevertheless, a validation study against measurements from large offshore wind farms remains to be done in order to assess TurbSim.Farm's ability to model power fluctuations.

TABLE OF CONTENTS

EXECUTIVE SUMMARY	4
TABLE OF CONTENTS	5
ABBREVIATIONS AND ACRONYMS	7
1 INTRODUCTION	8
1.1 CONNECTION TO WATEREYE'S SOLUTION	8
1.2 METHODOLOGY	9
2 PROPAGATION OF STOCHASTIC DYNAMICS IN WIND TURBINES	11
2.1 PROBABILISTIC STATE-SPACE MODEL	12
2.2 MONTE-CARLO WIND FARM SIMULATIONS	14
3 EFFICIENT MULTISCALE STOCHASTIC SIMULATIONS OF FARM-SCALE FLUCTUATIONS	16
3.1 FAST.FARM AND ITS LIMITATIONS	16
3.2 FARM-SCALE TURBULENCE MODELLING	17
3.2.1 <i>Farm-scale spectral modelling</i>	17
3.2.2 <i>Aggregation</i>	19
3.3 FARM-SCALE SYNTHETIC TURBULENCE GENERATION	22
3.3.1 <i>The modified Veers method</i>	22
3.3.2 <i>Cascaded generation</i>	22
3.3.3 <i>Implementation matters</i>	23
3.3.4 <i>Turbine-scale reconstruction</i>	23
3.4 RESULTS AND DISCUSSION	23
3.4.1 <i>Verification</i>	23
3.4.2 <i>Farm-scale case study</i>	25
4 AERO-SERVO ELASTIC SIMULATIONS	29
4.1 WIND FARM SIMULATIONS IN TIME-DOMAIN	29
4.1.1 <i>Effect of wakes and rotor dynamics on power fluctuations</i>	29
4.1.2 <i>Structural loads</i>	30
4.1.3 <i>Efficiency</i>	31
4.2 USE WITH STOCHASTIC STATE-SPACE MODEL	32
5 CONCLUSIONS	34
6 REFERENCES	35

LIST OF FIGURES

FIGURE 1. LINK BETWEEN WIND FARM CONTROL AND CORROSION THROUGH O&M PLANNING 9

FIGURE 2. UNCERTAINTY PROPAGATION. PROBABILISTIC MODELLING FOR UNCERTAINTY QUANTIFICATION..... 11

FIGURE 3. FLOW DIAGRAM OF THE PROBABILISTIC ANALYSIS TOOL USING A STATE-SPACE MODEL GENERATED WITH SINTEF’S STAS PROGRAM..... 12

FIGURE 4. FLOW DIAGRAM FOR TIME-DOMAIN MONTE CARLO SIMULATIONS. 15

FIGURE 5. MOTIVATION FOR THE DEVELOPMENT OF A MODULE FOR SYNTHETIC TURBULENCE GENERATION..... 17

FIGURE 7. STANDARD POINT-BASED, FARM-SCALE POINT-BASED AND FARM-SCALE AGGREGATED WIND SPECTRA. 20

FIGURE 8. POINT-BASED AND AGGREGATED COHERENCE..... 21

FIGURE 9. THREE-ROTOR DOMAIN FOR VERIFICATION..... 24

FIGURE 10. PSDS AND COHERENCES OF INTEREST FOR THE THREE-ROTOR DOMAIN FROM DIFFERENT IMPLEMENTATIONS OF TURBSIM, AVERAGED OVER SEEDS AND ROTORS/ROTOR PAIRS. 24

FIGURE 11. TURBINE-SCALE RECONSTRUCTION OF WIND FIELD..... 25

FIGURE 12. PSDS OF POWER FLUCTUATIONS FOR VARIOUS SPECTRAL MODELS. 26

FIGURE 13. SNAPSHOT OF TURBULENT WIND FIELD..... 27

FIGURE 14. STATISTICAL ANALYSIS..... 28

FIGURE 15. EFFECT OF WAKES ON POWER FLUCTUATIONS..... 30

FIGURE 16. VARIOUS LOADS ON SINGLE TURBINE WITH POINT-BASED (FF) AND AGGREGATED (HH) TURBULENCE REPRESENTATIONS..... 31

FIGURE 17. TRENDS IN THE OUTPUT SPECTRA WITH POWER COMMAND FROM D4.1 DLL..... 32

FIGURE 18. TIMESERIES OF FILTERED OBSERVED WIND SPEED FOR UPWIND AND DOWNWIND TURBINES 33

LIST OF TABLES

TABLE 1. OUTPUT OF THE PROBABILISTIC STATE-SPACE MODEL IMPLEMENTED AS DLL. 13

ABBREVIATIONS AND ACRONYMS

Abbreviations / Acronyms	Description
DLL	Dynamic Link Library
FFT	Fast Fourier Transform
MIMO	Multiple-input multiple-output
O&M	Operation and Maintenance
PSD	Power Spectral Density
RUL	Remaining Useful Lifetime
WT	Wind Turbine
WF	Wind Farm

1 Introduction

1.1 Connection to WATEREYE's solution

Turbine towers could theoretically fail and break down during their lifetime due to corrosion-induced cracks or accumulated structural fatigue. While wind farm control cannot prevent corrosion, the ability of wind farm control to reduce structural loads is investigated in a number of research projects worldwide with the goal of preventing the accumulation of fatigue. In theory, corrosion and fatigue are related through cracks initiated by corrosion and further developed by fatigue resulting from stress concentration. However, there is no simple heuristic between the two phenomena. First, the underlying physics depend on many unknown parameters and are hence totally case-dependent. Then, the corrosion-related assumptions and context considered in WATEREYE further discards the direct joint use of fatigue and corrosion in wind farm control:

WATEREYE focuses on uniform corrosion which rarely leads to cracks. The focus is on corrosion at the turbine tower, more specifically the corrosion in the splash zone. There, corrosion is normally prevented by protective coating and a corrosion allowance as described above. The expected lifetime of a coating system for offshore structures is 15-40 years.

If the coating is damaged, corrosion is initiated, and the corrosion allowance is consumed. Significant corrosion affects the wall thickness of the tower which again may change the structural properties and the stress (deflection and rotation) caused by the same level of structural loads (forces and moments). However, it is unlikely that uniform corrosion will have an effect on the structural properties of the tower within the turbines' design lifetime of approximately 25 years.

Thus, it is very unlikely that uniform corrosion is the root cause for a turbine tower breaking down. The more probable contribution of corrosion to such a failure is through cracks. However, cracks are out of the scope of WATEREYE.

While a direct link between corrosion and fatigue and hence wind farm control is hard to characterize, there exists an indirect link through maintenance planning, since the remaining useful life of wind turbines depends on both the corrosion-based and the fatigue-based cracks, on each of its components. Neither should eventually lead to failure, which necessitates monitoring and possibly repairs, orchestrated by optimal maintenance planning. This indirect link between corrosion and stochastic analysis of wind farms is shown in Figure 1.

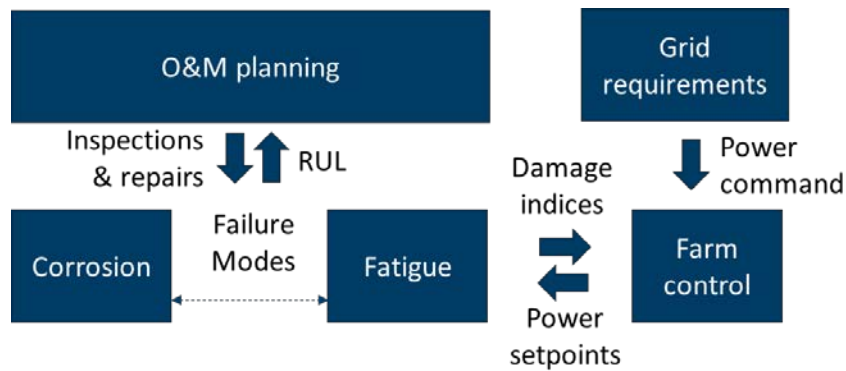


Figure 1. Link between wind farm control and corrosion through O&M planning

1.2 Methodology

Offshore wind turbines operate in an inherently stochastic and uncertain environment. Should it be because of the fluctuating nature of wind or of uncertainties in structural properties induced by limited access and measurement facilities, decision making can hardly be effective without probabilistic assessments. This implies analysing the effect of a number of possible combinations of occurrences, together with their joint probability distribution. This greatly increases complexity when compared to the deterministic approaches. While the latter –typically used to better understand underlying physics rather than real-life applications– can afford a high cost (computational, experimental), the former must use approximations and assumptions. Furthermore, offshore wind energy systems are particularly complex due to their intricate dynamics at various scales (from material to component to turbine to farm) and across disciplines. While academic deterministic studies typically isolate the different underlying phenomena to better understand them individually, system-level decision making needs to properly capture their interactions.

This study suggests an approach for multidisciplinary probabilistic decision making through the joint effect of fatigue- and corrosion-induced failures on O&M planning of offshore wind farms. While a turnkey comprehensive decision-making tool is out of reach, focus is set on the methodology of integrating aero-hydro servo analyses of wind *farms* (and not only their individual turbines) and subsequent fatigue damage calculations into medium-term decision making (weeks-ahead O&M planning), opening the way for combination with corrosion-related inspections or hypothetical repairs.

Emphasis is put on the ability to run these analyses in real time (provided sufficient computational power). Transferability is also a requirement, discarding the use of exceedingly costly high-fidelity simulations or proprietary softwares not usable by others to generate offline databases for later real-time use.

Given the ambitious objectives, scope restrictions had to be made, still guaranteeing the consistency of the methodology:

- Regarding the probabilistic aspect, focus is put on the stochastic aspect of wind turbulence. The chosen approach with Monte Carlo simulations would be directly applicable for

instance uncertainties in structural properties, wave loads, or even turbine layouts or control strategies, as long as they are characterized by a probability distribution.

- This report deals mostly with the aerodynamic part of the aero-hydro servo elastic response of wind farms. Wave loads (the *hydro* part) have been excluded. They can straightforwardly be included using more simulations and a long-term joint probability distribution of wave and wind parameters¹.
- As complexity conflicts with the real-time objective, the level of detail at the component level has to be limited. While significant information about global structural loads is captured, it is not sufficient for accurate fatigue damage calculations (the *elastic* part). Farm- and component-scales are hence decoupled with turbine-scale as an interface. This report focuses on farm scale, while component scale will be presented in D5.5.
- How to link wind farm control (the *servo* part) with O&M planning will be treated in D4.4.
- All aspects and scales will be assembled in D5.3 and exemplified in D5.5, gathering the WF management tools developed in WATEREYE.

2 PROPAGATION OF STOCHASTIC DYNAMICS IN WIND TURBINES

Wind energy is a variable source whose temporal variability even for a specific site covers wide ranges in space and time². Thus, the wind that approaches a wind turbine has not constant features but is subject to several statistical properties¹.

Neglecting spatial and temporal components for simplicity, turbulent wind can be decomposed into:

$$\tilde{U} = \bar{U} + U$$

Where \tilde{U} [m/s] is the wind speed in the longitudinal direction, \bar{U} [m/s] is the short-term mean wind speed and U [m/s] are zero-mean wind speed fluctuations¹. The wind speed in the lateral direction can be described similarly to the prevailing longitudinal direction. In addition, the wind speed \bar{U} changes with height.

Waves constitute another major environmental force that impacts offshore wind turbines. For many engineering applications including design studies, it is sufficient to assume steady-state environmental forces over certain periods¹. The offshore industry assumes often constant wave conditions over 3 hours, while the wind industry works with 10-min intervals of constant wind conditions. The estimation of component fatigue, however, may require more accurate models or frequent calculations to derive the estimated lifetime and make real-time control decisions.

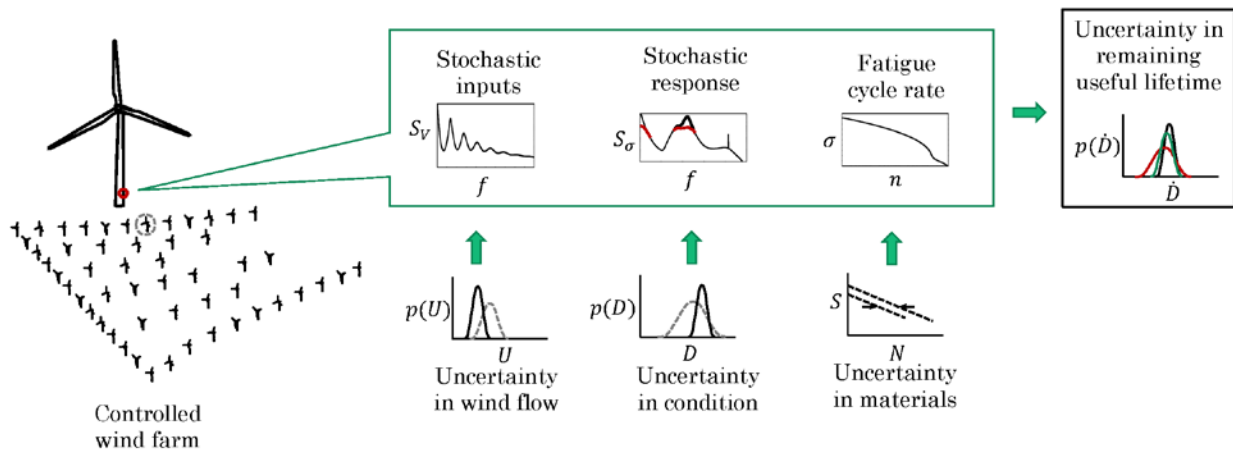


Figure 2. Uncertainty propagation. Probabilistic modelling for uncertainty quantification.

Figure 2 illustrates how wind and waves as stochastic inputs propagate through the system into the uncertainty in the estimated remaining useful lifetime of wind turbines. The uncertainty in the wind inflow (depicted by its probability density function $p(U)$) creates a stochastic input (represented by the wind speed spectrum S_v over the frequency f) at each wind turbine of the controlled wind farm. There is uncertainty in the condition of the wind turbine component in question (depicted by the damage probability density function $p(D)$) leading to a stochastic response of the material with the spectrum S_σ . This will be different for each component and the

loading history of that component. In addition, the effect that a certain mechanical load has on the material is uncertain and can differ due to the manufacturing process. The uncertainty of materials is illustrated by an S-N curve that connects the stress S to the number of cycles N at that stress that lead to failure. Thus, the stress σ caused by the load cycles n varies. This again leads to uncertainty of the remaining useful lifetime (RUL), summarized here as probability density function of the damage rate $p(\dot{D})$.

The underlying uncertainty should be considered when operational decisions are taken based on the estimated RUL. A probabilistic analysis can contribute to quantify the uncertainty and thus, provide decision support.

There are different methods to model and analyse stochastic system responses, see e.g. ^{1,3}. The general choice for such numerical analyses is between frequency domain and time domain approaches. An analysis in the frequency domain is computationally more efficient using a linearized model of the system. An analysis in the time domain has the advantage that nonlinear dynamics can be included. This is particularly relevant for wind turbines with their distinct nonlinearities in the control of the generator torque and the blade pitching³.

Two methods are introduced here that were used in WATEREYE.

2.1 Probabilistic state-space model



Figure 3. Flow diagram of the probabilistic analysis tool using a state-space model generated with SINTEF's STAS program.

In WATEREYE D4.1⁴, a probabilistic state-space model was implemented and provided as dynamic linked library (DLL) using SINTEF's STAS program. Figure 3 illustrates the data flow in the probabilistic analysis tool. The parameters for environmental conditions are input to the tool, and the output spectra of e.g., structural loads given as output. Input spectra are calculated for the environmental conditions using rotationally sampled turbulence spectra at the corresponding wind speeds and rotor speeds. Multiple-input multiple-output (MIMO) transfer functions derived from the linear state-space wind turbine model are used to calculate the output spectra.

The state-space model describes a bottom-fixed offshore wind turbine, and more specifically the statistical response of a wind turbine as a function of its operating conditions. The wind turbine response is generated from a multi-body aeroelastic model which also includes electrical

components, actuator dynamics, the turbine control system, and turbulent wind loads ^{5,6}. Linear state-space representations of the wind turbine at different operating conditions are collected in a DLL, which calculates the response at the input conditions by interpolation between pre-generated spectra of the response variables. In the present implementation, the output spectra are stored directly as part of the DLL to achieve a convenient file size. Computations involving the wind spectra and transfer functions are pre-calculated to save storage space.

The input variables include operational conditions (environmental conditions and external commands) and analysis parameters. The environmental variables are the effective wind speed v , the turbulence intensity I , the significant ocean wave height, and the ocean wave period. The external command is the requested electrical power \hat{P}_e . Analysis parameters are the tower elastic modulus, the number of frequencies to be analysed in the spectrum and a list of these output frequencies.

Table 1. Output of the probabilistic state-space model implemented as DLL⁴.

<i>Output</i>	<i>Description</i>	<i>Dimension</i>	<i>Units</i>
S_F	Nacelle fore-aft displacement spectrum	N_f	m^2/Hz
S_S	Nacelle side-to-side displacement spectrum	N_f	m^2/Hz
S_b	Blade root flapwise bending moment spectrum	N_f	$(\text{MNm})^2/\text{Hz}$
S_β	Blade pitch angle spectrum	N_f	rad^2/Hz

Table 1 presents the output spectra of the dynamic link library from WATEREYE D4.14. The spectra have the dimension N_f which is the number of the output frequencies f [Hz] defined in the input variables.

The nacelle displacements serve as measures of the tower loading, where the fore-aft displacement is aligned with the wind direction and the side-to-side displacement is perpendicular to it. The main driver for fatigue damage is the dynamic loading, not the static displacement. This is reflected in the spectra which show for each frequency the amplitude of the nacelle displacement if the tower is excited at that frequency.

Besides the nacelle displacement, the DLL returns the blade root flapwise bending moment and the blade pitch angle. These serve as measures for the loading of the rotor blades. The blade root flapwise bending moment describes the structural loads that can cause fatigue of the blade material, the blade pitch angle describes the usage of the blade pitch actuator which is subject to wear.

More details about the probabilistic state-space implementation including an example application can be found in the documentation accompanying WATEREYE Deliverable D4.1. The provision as DLL is an add-on to support interoperability of different tools. However, the presented method is more general and not restricted to that format.

The general method applies spectral analysis which implies a linearized dynamic model with Gaussian statistics. This has the advantage that Gaussian probabilistic estimates of the wind turbine response variables can be quickly computed from the pre-generated spectra. These fast estimates of the response statistics including important load components and of the effect of derating the power production enable better informed, real-time operational decisions. Moreover, the fatigue cycle accumulation rate can be calculated from a spectrum of the signal, thereby enabling to estimate the damage-equivalent loads and other fatigue measures. The latter is possible because the integral under the spectrum of the analysed variable equals the standard deviation of that variable.

2.2 Monte-Carlo wind farm simulations

While the frequency domain offers a powerful way of propagating uncertainty, the assumption of linearity has limitations:

- Wind turbine controls are inherently nonlinear.
- It implicitly assumes Gaussian probability distributions. Although this may be reasonable for stochastic processes such as wind and waves, it may be overly simplifying the characterization of uncertainty in structural properties.
- Frequency-domain estimation of fatigue damage is challenging.
- Comprehensive (mid-fidelity) analytical state-space models of wake flow and dynamics are hard to construct due to the number of states in play. The analyses run with STAS in 2.1 only consider the ambient (not the disturbed) wind field.
- Transferability is a focus, and comprehensive analytical state-space models tend to be exceedingly complex, and their usage must be adapted case by case. They are hence hardly usable by others without deep knowledge of the tool.

Consequently, a more traditional time-domain approach has been considered. Propagating uncertainties is made by running a number of simulations corresponding to samples (also called realizations, or seeds, for stochastic processes) taken from a probability distribution describing the stochastic or uncertain underlying process, known as Monte-Carlo simulations. Quantities of interest are then derived by averaging between realizations and corresponding uncertainty may

be analysed by cross-analysing realizations¹. The process is illustrated in Figure 4, in contrast with Figure 3.

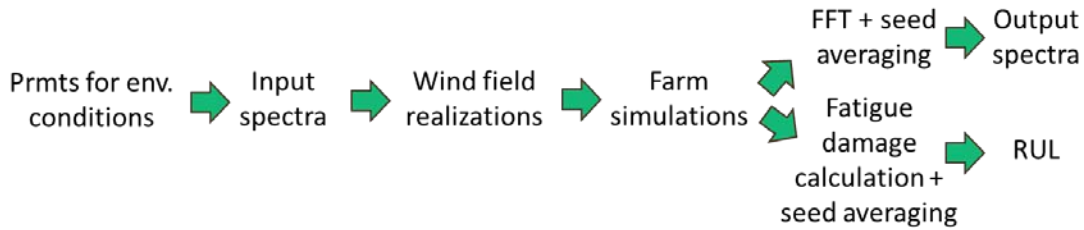


Figure 4. Flow diagram for time-domain Monte Carlo simulations.

The simulation tool presented in this report is based on mid-fidelity engineering models put into a platform efficiently running multiple simulations corresponding to different wind field realizations. It consists of an existing wind farm simulator, an additional module and a platform for efficient computation. The module has been partly developed in WATEREYE and gives more realistic farm-level turbulence fluctuations in wind farms, laying the ground for development and testing of farm-wide control strategies and their effects on rest-of-life assessments.

Details about the developed tool are explained in Section 3. Its use in a probabilistic setting is explained in Section 4.

3 EFFICIENT MULTISCALE STOCHASTIC SIMULATIONS OF FARM-SCALE FLUCTUATIONS

3.1 FAST.Farm and its limitations

NREL's FAST.Farm⁷ is a wind farm simulation tool based on the aero-hydro-servo elastic wind turbine code OpenFAST, widely used in the wind energy community. It is chosen for the following reasons:

- Mid-fidelity: engineering model with optimal ratio between computational time and accuracy, standardly used to design offshore structures. Fidelity is not compromised when compared to simplified analytical models (used for instance in optimization or multidisciplinary couplings); Computational time is decent compared to high-fidelity modelling (CFD).
- Multiscale approach: all turbines are simulated in parallel (one OpenFAST instance each) and wrapped up at farm level where wakes are modelled and added to the flow. This contrasts with other tools where approximations are made at the turbine level to meet computational efficiency requirements.
- Open-source philosophy for transferability and collaboration
- Computational efficiency (implemented in compiled language, compared with other tools implemented in interpreted language)

A design requirement for the wind farm simulation tool is the ability to encompass wind farm controllers balancing out power fluctuations and structural degradation between turbines. For this, farm level wind turbulence with correct correlation between turbines is needed. Additionally, wake meandering is important for loads and needs to be properly modelled. As it is driven by lateral turbulent vortices along the wake's trajectory, the turbulent wind field should not only be modelled at the turbines, but also between them.

Although FAST.Farm is virtually able to simulate large wind farms with sufficient efficiency for Monte Carlo simulations, the ambient turbulent wind field it uses as input appears to be a bottleneck. There are originally two options to model the wind field in FAST.Farm. The first is a rough extension of turbine-scale wind fields using NREL's synthetic turbulence generation tool

TurbSim; The second is based on CFD modelling. They are presented in Figure 5. None of them is appropriate for Monte Carlo simulations of farm-level coherent (correlated) turbulent wind fields.

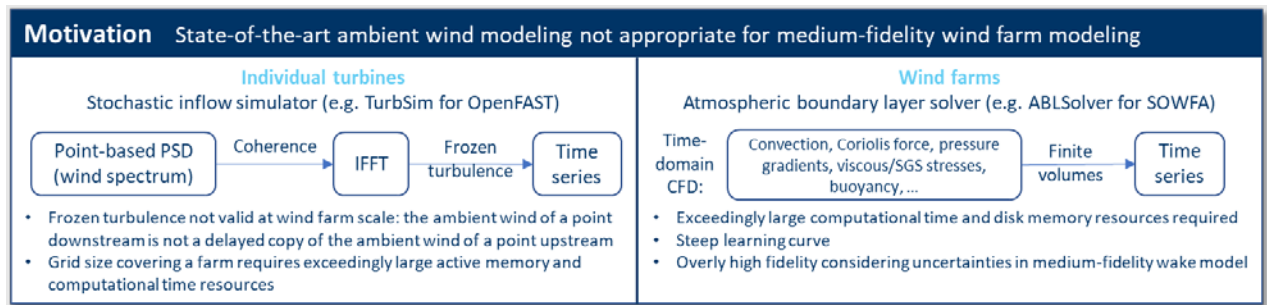


Figure 5. Motivation for the development of a module for synthetic turbulence generation.

The solution developed in WATEREYE may be thought as an extension of the stochastic inflow simulator for synthetic turbulence generation (left-hand option on the figure) from turbine level to farm level.

It is based on the concept of aggregated -or space-averaged- wind speed. In practice, global aerodynamic loads (e.g. rotor thrust) and power are driven by rotor-averaged wind velocities². Current models for wake dynamics use space-averaged velocities⁸. Since we actually don't need point-based velocities for our purpose, the idea is to process point-based models to yield aggregated counterparts efficiently upfront. Then, instead of point-based velocities on a fine-meshed grid, we model aggregated values on a much coarser grid, effectively reducing the number of degrees of freedom and hence drastically improving computational efficiency.

The idea is not new and was originally suggested by Sørensen^{9,10}. The work done in WATEREYE is an adaptation for use in FAST.Farm, in particular for wake dynamics, among other functional and computational improvements.

A summary of the theory behind farm-scale aggregated turbulence modelling is given in Section 3.2, and its implementation for synthetic turbulence generation in Section 3.3. Further details may be found in the corresponding scientific publication¹¹.

3.2 Farm-scale turbulence modelling

3.2.1 Farm-scale spectral modelling

3.2.1.1 Wind spectrum

Modelling of fluctuating wind loads for engineering purposes is conveniently done in the frequency domain through a wind spectrum. It gives the power spectral density of wind velocities at one point in space, based on historical site measurement data, typically from met masts. The data is processed to fit parametrized models as function of mean wind speed and other parameters

describing terrain (e.g. surface roughness) and meteorological conditions (e.g. atmospheric stability).

For wind energy, a commonly used spectrum used in the IEC standard is the Kaimal spectrum reading

$$S_{IEC}(f) = I\overline{U_\infty} \frac{2L}{1 + 6\frac{L}{U_\infty}f}$$

With only the length scale L , the mean wind speed at hub height $\overline{U_\infty}$ and the turbulence intensity I as parameters. This model is used for its simplicity but has been widely discussed in the literature. Among others, the effect of other parameters like surface roughness and atmospheric stability is pointed out.

An important assumption behind these spectrum models is the so-called spectral gap between microscale (periods up to 10 min) and mesoscale (4 hours and above), with least energy at about 1 hour. This defines a distinction between diurnal and semi-diurnal weather fluctuations on the one hand and turbulence on the other hand. This explains the 1-h resolution for weather forecast and hindcast data giving mean wind speed and direction, and the 10-min duration for turbulent wind simulations used for structural design of wind turbines, specified in design standards¹². However, measurement data from wind farms show no such spectral gap^{13,14,15}. While turbulent fluctuations of periods of tens of minutes to hours have traditionally not been of much engineering interest, they become essential when it comes to power fluctuations of large wind farms. Therefore, farm-scale spectra need to be used, as those developed by Viguera-Rodriguez et al.¹³ and Cheynet et al.¹⁵. While the former is based on extensive data from multiple wind farms (and for this reason it will be used throughout this report), the latter is more elaborated and incorporates the effect of atmospheric stability, showing the partial validity of the spectral gap.

The model of Viguera-Rodriguez et al. simply adds low-frequency content to the original Kaimal spectrum, viz.

$$S(f) = S_{IEC}(f) + S_{LF}(f)$$

It is illustrated in Figure 6 for a mean wind speed of 10 m/s using the IEC 61400-1 Ed.3 standard with turbulence class B to define turbulence intensity and length scale¹². Note: The spectrum is scaled by frequency as standardly done for visualization purposes, which might give a false impression of negligible low-frequency content.

3.2.1.2 Coherence

In addition to the wind spectrum which provides a temporal characterization of turbulence, a spatial characterization is used for structures like wind turbines which need a proper description of the correlation between wind speeds across its swept area (if there was no spatial correlation, all velocities would be independent, and their sum would statistically be zero, leading to *no* power or thrust fluctuations). This correlation, or *coherence*, is what characterizes the shape of turbulence vortices. Its derivation from field data is more complicated than for the wind spectrum because it

needs measurements from different spatial locations. Furthermore, it is typically anisotropic, so the various spatial locations should cover the three directions.

As a result, coherence models used in design standards are not applicable for farm scale: as data is acquired from anemometers on met masts, only a characterization of coherence in the vertical direction is feasible, with limited span. The along-wind direction is encompassed by assuming vortices are simply advected downstream without change over time (the so-called Taylor's frozen-turbulence assumption). This is valid over short distances/time intervals, but not to study power fluctuations on large wind farms.

To model farm-scale coherence, Vigueras-Rodriguez et al. (2012)¹⁶ used data from turbine nacelle-mounted anemometers for the same wind farms and measurement period as for the spectrum model in ¹³. Special focus is put on the along-wind direction, which had never received attention before.

3.2.2 Aggregation

3.2.2.1 Rotor-averaged wind spectrum

It is well known that wind turbine -like helicopter- rotors may be represented as actuator discs when it comes to modelling their global aerodynamics. Rotor aerodynamic loads (e.g. thrust) and power may be computed by means of quasi-static coefficients varying with tip-speed ratio $\lambda = \frac{\Omega R}{U_\infty}$ (with Ω the rotor speed, R the rotor radius and U_∞ the incoming undisturbed wind speed) and pitch angle β :

$$\begin{aligned} Thrust &= C_T(\lambda, \beta) \frac{1}{2} \rho A U_\infty^2 \\ Power &= C_P(\lambda, \beta) \frac{1}{2} \rho A U_\infty^3 \end{aligned}$$

with possible encompassment of inflow (near-wake) dynamics and yaw misalignment.

In this representation, U_∞ is the average wind speed over the rotor's swept area, viz

$$U_\infty(t) = \frac{\int_\Omega u(t) d\Omega}{\int_\Omega d\Omega}$$

where u is the point-based wind speed and Ω is the integral domain (here the rotor's swept area).

In order to characterize it from the point-based wind spectrum and coherence function, an average of the latter *over all possible combinations of points on the swept area* is made, leading to a transfer function H (the so-called admittance function) from point-based to rotor-averaged (or *aggregated*) wind spectrum:

$$S_{agg}(f) = H^2(f)S(f)$$

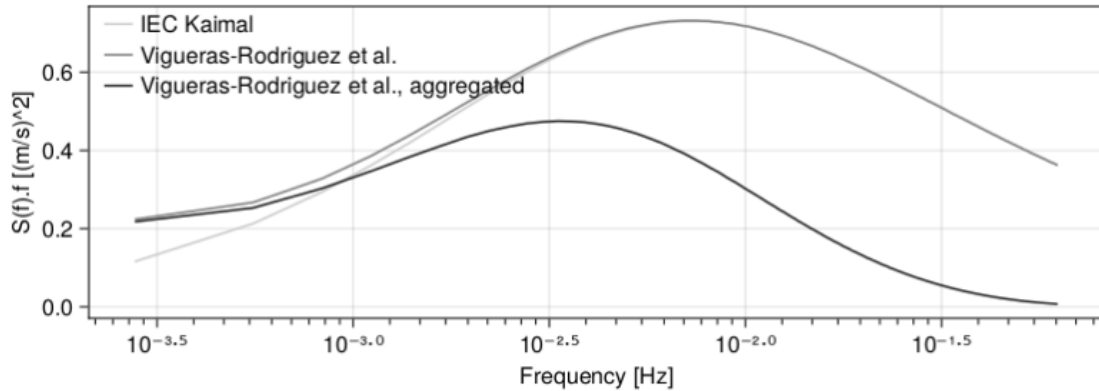


Figure 6. Standard point-based, farm-scale point-based and farm-scale aggregated wind spectra.

Wake dynamics may also be divided in different scales. As far as farm-scale fluctuations are concerned, spatially averaged values of the turbulent wind field (i.e. large turbulent vortices) drive wake advection and meandering but also affect wake recovery (velocity-deficit evolution), essential for power modelling. Smaller-scale turbulence is modelled theoretically independently on the ambient wind field⁷, hence only averaged values are needed in practice. The state of the art is to use a high-resolution wind field on a fine grid mesh representing point-based wind speeds, and then averaged them in the time domain during farm simulation. The approach suggested here is to make this averaging in the frequency domain upfront readily modelling an aggregated turbulent wind field between turbines for use in wake dynamics computations. To do so, an aggregated grid is defined, with each grid point corresponding to a 3D averaging domain, or *cell*, of size of same order of magnitude as the wake (or rotor) diameter. As for its rotor-based counterpart, a cell-based aggregated spectrum is devised.

3.2.2.2 Aggregated coherence

The point-based coherence function may then be averaged over all combinations of points *between* cells rather than on the same cell, yielding an *aggregated coherence function* as function of distance between cell centres. This characterizes the coherence between aggregated wind speeds, in essence a low-pass filtered version of its point-based counterpart averaging out small, high-frequency turbulence vortices.

If one is only interested in turbine-to-turbine coherence and not wake dynamics (as in the original work of Sørensen et al.), distances are so large that aggregated coherence is typically well described by its hub-to-hub value, hence point-based and aggregated coherences coincide.

Figure 7 illustrates the difference between point-based and aggregated coherences for a frequency of 0.006 Hz, cell size of 200m x 80m, mean wind speed of 10m/s. x is the along-wind direction, and y the transversal direction.

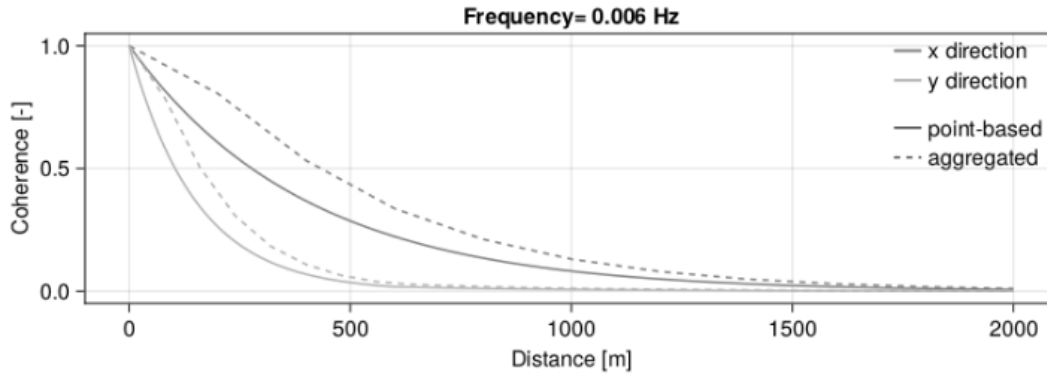


Figure 7. Point-based and aggregated coherence.

3.2.2.3 Shear components

While rotor-based aggregated along-wind wind speeds drive power and thrust and cell-based aggregated transversal wind speeds drive wake dynamics, loads need a finer description of the wind field. In this report, we suggest augmenting the aggregated wind field to provide an indicator for blade loads trends, to be calibrated/further analysed in point-based turbine-scale simulations. The bulk of blade and drivetrain loads comes from spatial variations in the wind field originating from wind profile, tower shadow and turbulent vortices of size comparable to that of the rotor. While the two former ones are readily included, the latter may be approximated by linear variations across the rotor, or *linear shears*:

$$s_y = \frac{\int_{\Omega} zu d\Omega}{\int_{\Omega} z^2 d\Omega}, s_z = \frac{\int_{\Omega} -yu d\Omega}{\int_{\Omega} y^2 d\Omega}$$

Where s_y and s_z are the vertical and horizontal shears and z and y are the vertical and horizontal position with respect to hub, respectively.

Similarly, to the aggregated wind spectrum, this averaging may be done in the frequency domain through a weighted average of the coherence function, yielding new admittance functions and spectra. In theory, the correlation of shears between turbines should be modelled by use of a corresponding aggregated coherence function. In practice, the large distances between turbines yield no correlation, so shears may be generated independently for each turbine.

Linear shears can readily be used as input in actuator-disc (or hub-height) representations of the wind field in FAST.Farm, effectively enriching the wind field to give an indicator about blade and torsional loads.

3.3 Farm-scale synthetic turbulence generation

3.3.1 The modified Veers method

3.3.1.1 Generation of correlated stochastic processes

Generating timeseries from spectral representation (power spectral density (PSD) and coherence) is standard for correlated processes such as wind fields or earthquakes. It has been adapted to wind turbine applications by Veers whom the method is named after ¹⁷. The idea is to look for a wind field satisfying the relation:

$$S_{agg}\mathbf{\Gamma} = \mathbf{U}\mathbf{U}^H$$

With $\mathbf{\Gamma}$ the aggregated coherence matrix ($S_{agg}\mathbf{\Gamma}$ being the aggregated cross-spectral matrix) between points at which the process is to be generated. \mathbf{U} is the vector of Fourier coefficients of aggregated wind velocities, related to the wind speed timeseries at each point by the Fourier transform and its inverse.

This is achieved *in the stochastic sense* by using

$$\mathbf{U} = \sqrt{S_{agg}} \mathbf{L} \mathbf{\Phi}$$

With \mathbf{L} the Cholesky factor of $\mathbf{\Gamma}$ reading $\mathbf{L}\mathbf{L}^H = \mathbf{\Gamma}$ and $\mathbf{\Phi}$ a vector of unitary complex numbers with random phase angles reading $\langle \mathbf{\Phi}\mathbf{\Phi}^H \rangle = \mathbf{I}$ with \mathbf{I} the identity matrix and $\langle \rangle$ the averaging operator between stochastic realizations, yielding $\langle \mathbf{U}\mathbf{U}^H \rangle = S_{agg}\mathbf{\Gamma}$

3.3.1.2 Advection

As suggested by Sørensen et al., the advection of turbulent vortices with the mean wind speed may be represented through the imaginary part of the coherence, $\mathbf{\Gamma}$ being the real part. It is in essence a time shift, which might be represented by a phase shift matrix $\mathbf{\Theta}$ between points as function of wind speed, frequency, and along-wind distance. Simplifying the method from ⁹, we use here the results of Huang et al. (2013)¹⁸ to decouple the real and imaginary parts in the solution, viz.

$$\mathbf{U} = \sqrt{S_{agg}} (\mathbf{L} \odot \mathbf{\Theta}) \mathbf{\Phi}$$

with \odot the Hadamard (elementwise) product.

The frozen-turbulence assumption used in the Mann and Veers methods implicitly uses this complex coherence representation by using $\mathbf{\Gamma} = \mathbf{L} = \mathbf{I}$ in the along-wind direction, leading to an equivalence between along-wind and time variations.

3.3.2 Cascaded generation

In section 3.2.2 we have defined the concepts of rotor-based and cell-based aggregation. Now, how do we generate a consistent aggregated wind field that jointly satisfies a rotor-aggregated

cross-spectral matrix between turbine points and a cell-aggregated cross-spectral matrix between grid points? We suggest a two-stage approach: first a rotor-based realization \mathbf{U}_T at turbine points, then a cell-based realization \mathbf{U}_G at grid points that is consistent with \mathbf{U}_T .

Let \mathbf{P}_T be an interpolation matrix mapping grid points to turbine points. We are seeking for \mathbf{U}_G satisfying

$$(1) \quad \mathbf{U}_T = \mathbf{P}_T \mathbf{U}_G = \sqrt{S_{agg_G}} \mathbf{P}_T (\mathbf{L}_G \odot \boldsymbol{\Theta}_G) \hat{\boldsymbol{\Phi}}_G = \mathbf{G}_G \hat{\boldsymbol{\Phi}}_G$$

which is obtained by carefully choosing $\hat{\boldsymbol{\Phi}}_G$ as

$$\hat{\boldsymbol{\Phi}}_G = \mathbf{G}_G^+ \mathbf{U}_T + (\mathbf{I} - \mathbf{G}_G^+ \mathbf{G}_G) \boldsymbol{\Phi}_G = \mathbf{G}_G^+ \mathbf{U}_T + \mathbf{G}_G^- \boldsymbol{\Phi}_G$$

with $\mathbf{G}_G^+ = \mathbf{G}_G^H (\mathbf{G}_G \mathbf{G}_G^H)^{-1}$ the Moore-Penrose pseudo inverse matrix of \mathbf{G}_G , \mathbf{G}_G^- its null space matrix and $\boldsymbol{\Phi}_G$ a vector of unitary complex numbers with random phase angles satisfying $\langle \boldsymbol{\Phi}_G \boldsymbol{\Phi}_G^H \rangle = \mathbf{I}$. Using the properties of the pseudo-inverse matrix¹⁹, it can be proved that (1) holds and $\langle \hat{\boldsymbol{\Phi}}_G \hat{\boldsymbol{\Phi}}_G^H \rangle = \mathbf{I}$, showing the validity of the solution for random process generation.

Note that this approach may also be used to reconstruct a wind field around turbines from wind speeds calculated back from the turbines' measured responses (using turbines as observers).

3.3.3 Implementation matters

Although turbulence aggregation looks promising to reduce the number of degrees of freedom, the gain in efficiency may be compromised by (1) aggregated coherence calculations involving costly sextuple integrals and (2) indefinite coherence matrices while Cholesky factorization needs positive-definite matrices. Methods to circumvent these problems are presented in the associated paper¹¹.

3.3.4 Turbine-scale reconstruction

A method to reconstruct high-resolution point-based wind fields from aggregated ones has also been devised. It is based on the same principle as in section 3.3.2 using pseudo-inverse matrices, see ¹ for details. This way, *correlated* turbine-scale simulations may be run for a selection of turbines consistently with results of farm-scale simulations.

3.4 Results and discussion

3.4.1 Verification

A comparison between NREL's point-based synthetic turbulence generation code TurbSim²⁰ and its farm-scale counterpart developed here, called TurbSim.Farm, is made. A three-rotor grid as illustrated in Figure 8 is used in TurbSim, corresponding to three turbine points in TurbSim.Farm, aligned in the cross-wind (y) direction.

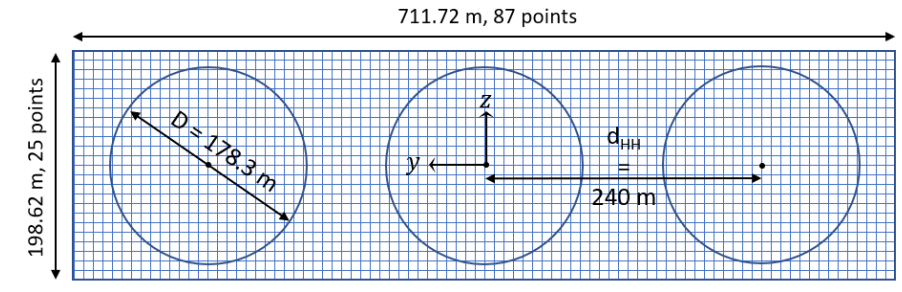


Figure 8. Three-rotor domain for verification

Ten realizations are run in each code. Results are shown in Figure 9, where *Freq. domain* refers to results from TurbSim.Farm (frequency-domain averaging) and *Time domain* from TurbSim. The right-hand plot shows the aggregated coherence between two adjacent rotors. The good match (small discrepancies being attributed to statistical and integration errors) validates the derivation and implementation of aggregated turbulence generation.

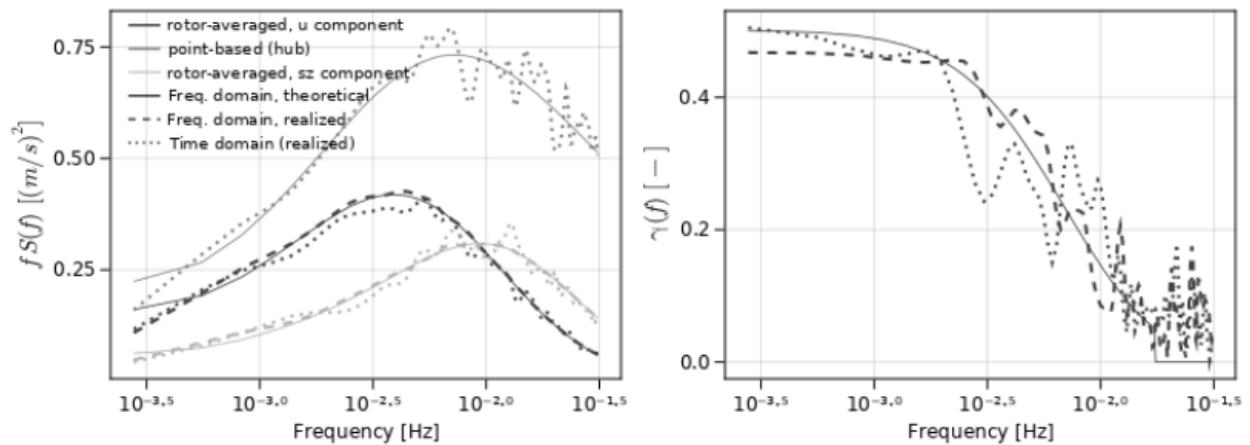


Figure 9. PSDs and coherences of interest for the three-rotor domain from different implementations of TurbSim, averaged over seeds and rotors/rotor pairs.

Turbine-scale reconstruction as introduced in Section 3.3.4 is verified in Figure 10, using a modified version of TurbSim¹. The right-hand plot shows a comparison between reconstruction and original TurbSim, for both the point-based wind speed at hub and the integral over blades assuming a constant rotor speed (note the peak at three times the rotor frequency known as 3p frequency), showing the consistency of the reconstruction.

¹ TurbSim is open-source and used as a base

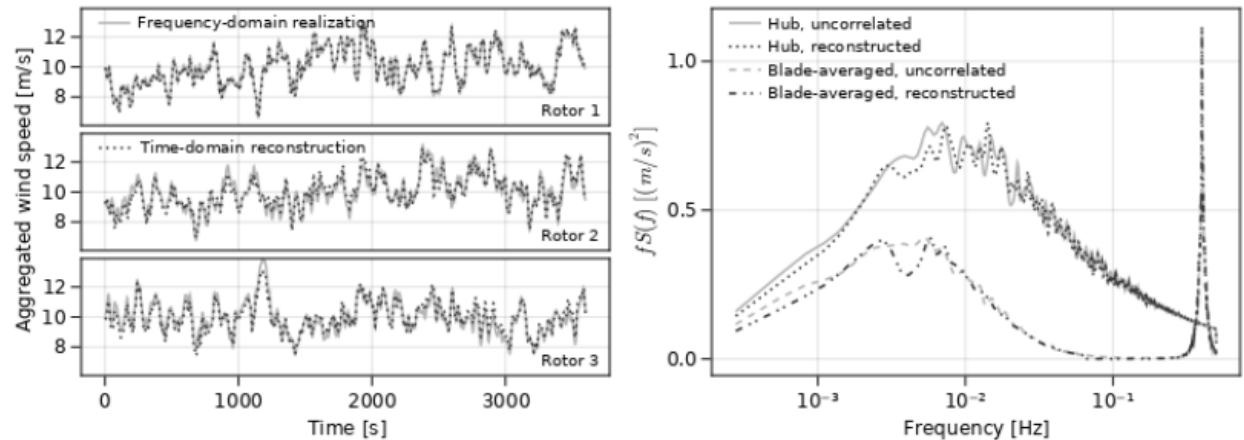


Figure 10. Turbine-scale reconstruction of wind field

3.4.2 Farm-scale case study

3.4.2.1 Effect of modelling errors and farm-scale improvements

If it was to be used consistently at farm scale, TurbSim would need about 10^5 more points/timesteps than TurbSim.Farm (about 20 for discretization in each direction in space, times 20 for time discretization). Frozen turbulence and an excessively coarse discretization in the inter-turbine domain (grid points) somewhat reduce this difference, but induce errors in correlation modelling. These errors corresponding to improvements in TurbSim.Farm are illustrated in this section, in addition to the effect of farm-scale spectral models.

The total control reference wind power plant consisting of 32 DTU 10MW reference turbines placed in a staggered pattern²¹ is used, with a wind speed of 10 m/s and turbulence class B¹². A direction of 0 degrees is chosen, so turbines the 16 downwind turbines stand in the wake of the 16 upwind ones, by pairs. Wakes are however not included in the flow simulation (we are directly interpreting results from TurbSim.Farm in this section for simplicity, not its use in FAST.Farm). As will be illustrated in Section 4.1.1, wakes affect the quantitative results but not the trends.

Power fluctuations are quantified by using the actuator-disc relationship introduced in 3.2.2.1.

Results are shown in Figure 11. *Full farm scale* is the reference with all improvements introduced in Sections 3.2 present. Other curves correspond to one improvement removed at a time (the others being present). *Frozen turbulence* has been introduced earlier. *Turbine-scale wind spectrum* refers to the standard IEC Kaimal spectrum. *No-farm scale coherence* considers the aggregated wind spectrum, but turbine points are uncorrelated.

It is seen that turbine-scale spectra and lack of farm-scale coherence yields significant errors in low frequencies (periods of 5 minutes and above), which is consistent with the 10 minutes duration of turbine-scale simulations. Frozen turbulence on the other hand shows to be inherently inappropriate, despite being the state of art. The oscillations observed in the PSD are actually as expected: the time shift between upwind and downwind turbines will translate into a phase shift

as function of frequency; peaks in oscillations correspond to a phase multiple of 2π , when the same turbulent vortex hits upwind and downwind turbines simultaneously.

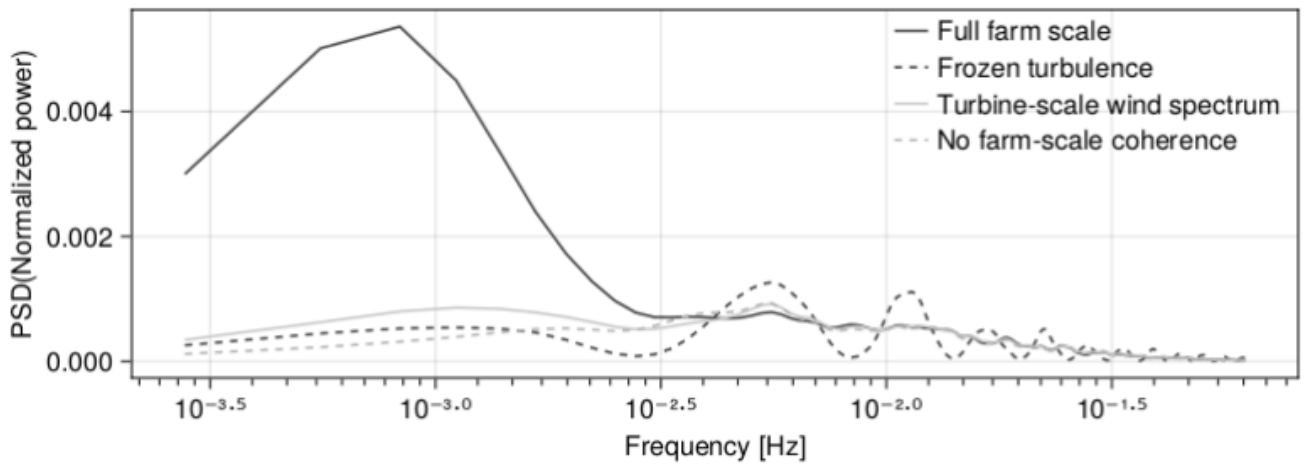


Figure 11. PSDs of power fluctuations for various spectral models.

3.4.2.2 Inter-turbine domain (grid points)

Cell-based aggregation and synthetic turbulence generation at grid points in a second stage account for most of the computational time and development efforts. Its results are however not interpretable directly from TurbSim.Farm, and make sense only through a model for wake dynamics as in FAST.Farm.

The discretization used was 200m in the along wind direction (x) and 80m in the cross-wind direction (y). The ratio between the two stems from anisotropy in coherence (it decays much faster in the y direction). In the vertical direction (z), only one aggregation cell is considered (which may be insufficient to capture vertical meandering). The wind field is then expanded according to the wind profile. Sensitivity studies on discretization are left as further work. A snapshot of the turbulent wind field is shown in Figure 12 with turbine layout present. Variations between turbines from smaller vortices are observed and cancel out when averaged over the number of turbines. Larger coherent structures (vortices) are also present and explain in a more visual way the low-frequency power fluctuations seen in Figure 11.

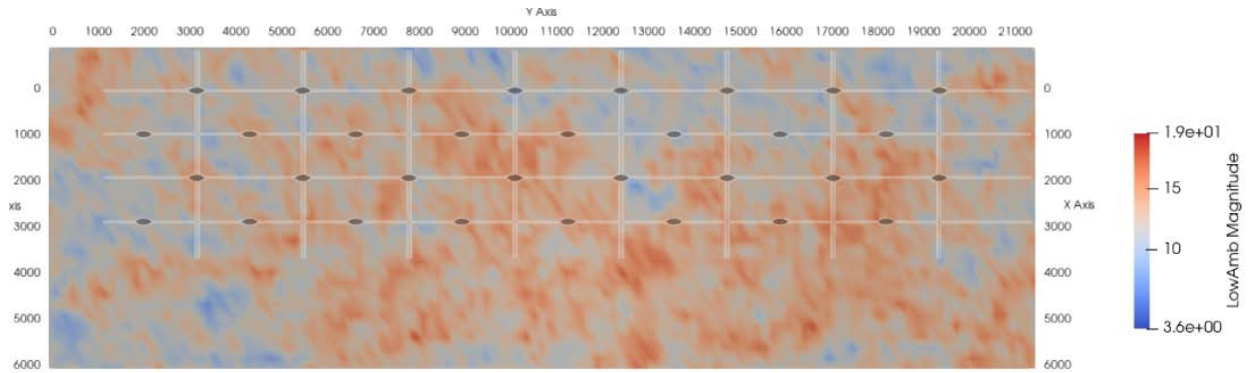


Figure 12. Snapshot of turbulent wind field.

3.4.2.3 Efficiency

The efficiency of the simulation may be measured by the ratio between CPU time and simulated time, and the percentage of CPU time that can be parallelized. The current implementation of TurbSim.Farm for the case study considered here shows a CPU time/simulated time ratio of about 1 per wind speed component (along-wind, cross-wind and vertical), meaning that it would run at about real time if each wind speed component ran on a different core, if implementation allows it.

3.4.2.4 Statistical analysis

The probabilistic analysis tool devised in this report is based on random phase angles in the stochastic wind field. Monte Carlo simulations are then run based on phase angles sampled from a uniform distribution using random seeds. It is possible to compute various statistical quantities (e.g. statistical moments) from these simulations, the simplest and most important being the mean value.

Figure 13 shows an example of the evolution of the mean value of farm-scale PSD as function of number of realizations (put in random order among many possible combinations), with plus/minus the standard deviation for 10 realizations in dotted lines. It is seen that low-frequency fluctuations justify the use of 10 seeds, where only few periods are included in one realization.

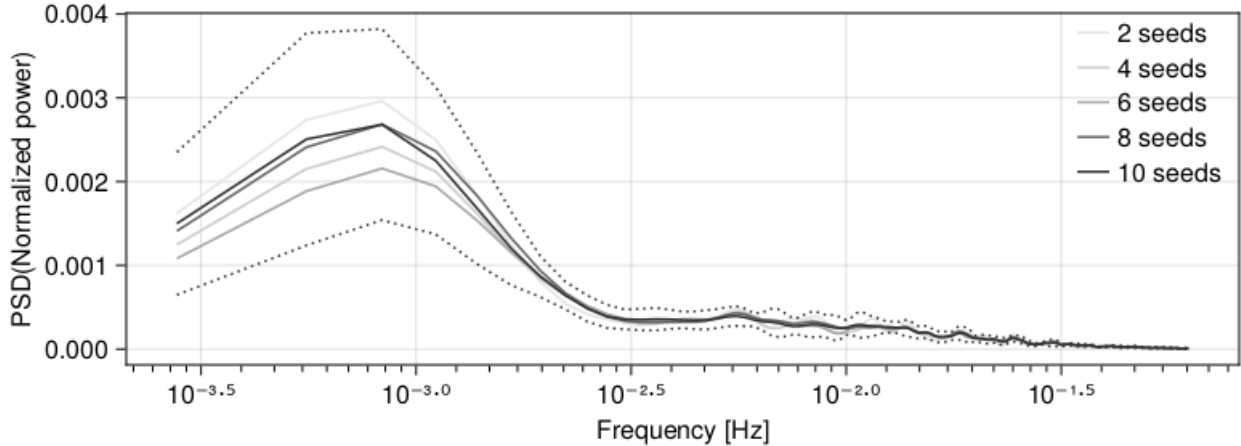


Figure 13. Statistical analysis

4 AERO-SERVO ELASTIC SIMULATIONS

In Section 3, focus was put on power fluctuations because of its dominant position in wind farm control. However, fatigue damage is induced by structural loads, which also need to be described in a stochastic sense to be propagated up to O&M planning.

This section aims to

- Use the wind field generated with TurbSim.Farm as described in Section 3 in mid-fidelity farm simulations including turbine and wake dynamics, focusing on the stochastic aspect
- Make a bridge over farm-scale simulations and frequency-domain analytical approach used in ⁴

4.1 Wind farm simulations in time-domain

Stochastic FAST.Farm simulations of the TotalControl reference wind power plant have been run with input from TurbSim.Farm. Wake properties have been kept as default. The wind turbine controller used is the DTU wind energy controller²².

4.1.1 Effect of wakes and rotor dynamics on power fluctuations

The simplified approach in Section 3.4.2 did not consider wakes, nor turbine dynamics (the tip speed ratio and pitch angle used in the calculation of the power coefficient was fixed to mean value). Neglecting the latter is a valid assumption when looking at the low-frequency range where most fluctuations are seen. The former, however, is expected to affect power fluctuations through a change in mean wind speed for downwind turbines combined with the nonlinear (cubic) relationship between power and wind speed on downwind turbines.

Figure 14 shows the PSD of power fluctuations directly from TurbSim.Farm with power coefficient, and from FAST.Farm (1) with wakes, (2) without wakes and (3) without wake dynamics, i.e. without turbulent fluctuations (using steady mean wind speed) in the inter-turbine domain (grid points). All in all, wakes have a limited effect on power fluctuations with respect to the significant uncertainties in low-frequency turbulence modelling. Still and interestingly, it is better not to include wakes at all (and hence use TurbSim.farm directly) than to include wakes in a quasi-steady fashion, removing then turbulent mixing in the wake's velocity-deficit evolution (also known as wake recovery). The latter greatly overestimates the decrease in mean wind speed on downwind turbines, and hence the power fluctuations

Wake meandering could also potentially affect power fluctuations on downwind turbines, although it has mostly been deemed important for loads. There, it should be noted there that wake meandering is likely underestimated in the low-frequency range: Sørensen's farm-scale spectral model has only been derived for the longitudinal component, the transversal component still using a turbine-scale model. However, according to the model of ¹⁵, the transversal components show an even more significant (relatively) low-frequency content than its longitudinal counterpart.

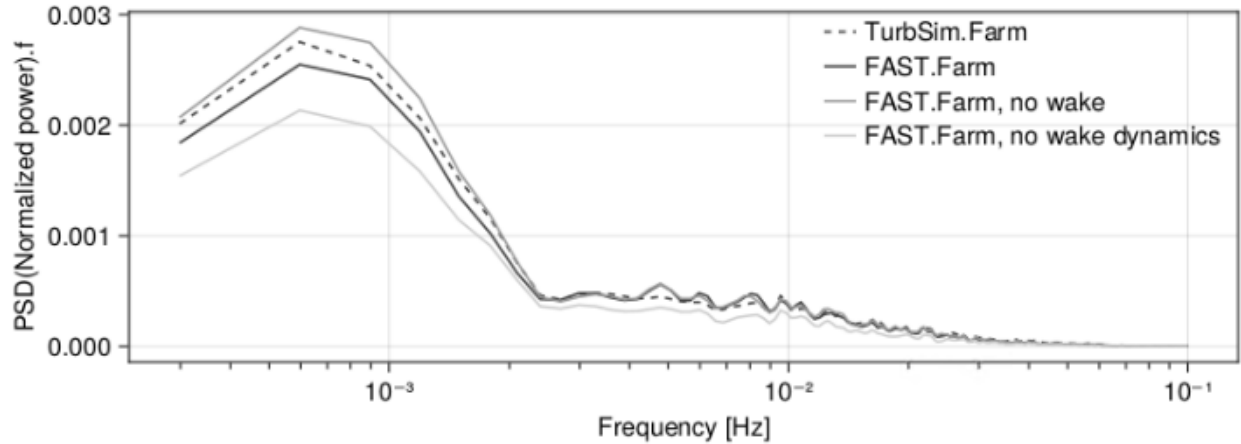


Figure 14. Effect of wakes on power fluctuations

4.1.2 Structural loads

The present farm simulations are not aimed to accurately model turbine dynamics due to the aggregated turbulence representations. Still, this representation (especially with the inclusion of linear shears) should give an indication about the difference between turbines across the wind farm in level of loading and hence in fatigue damage rate, to be used for control rather than for design.

Figure 15 compares results from OpenFAST simulations (on single turbine) using (1) aggregated wind speed representations with and without linear shears (only one realization each) and (2) the average between 10 realizations of point-based representations reconstructed from the aggregated one as presented in Sections 3.3.4 and 3.4.1.

It is seen that turbulence aggregation is able to accurately preserve load modelling up to frequencies of the order of 0.1 Hz (which corresponds to the time constant of the admittance function for rotor averaging). This will accurately inform the wind farm controller about current loading in the frequency range where power fluctuations are important, but not for instance accurately inform about fatigue damage in the presence of added wake turbulence.

As expected, shears show to be important for quantities driven by in-plane forces or out-of-plane rotor aerodynamic loads, such as the torsional (yaw) moment, as well as for 1p blade loads.

3p loads (peaks at ~ 0.4 Hz in the figure) are not accounted for in the current implementation of aggregated turbulence, but may be included to some extent in further development using azimuthal expansion of the rotationally sampled wind field, as done to include 3p (and harmonics) power fluctuations in grid models¹⁰.

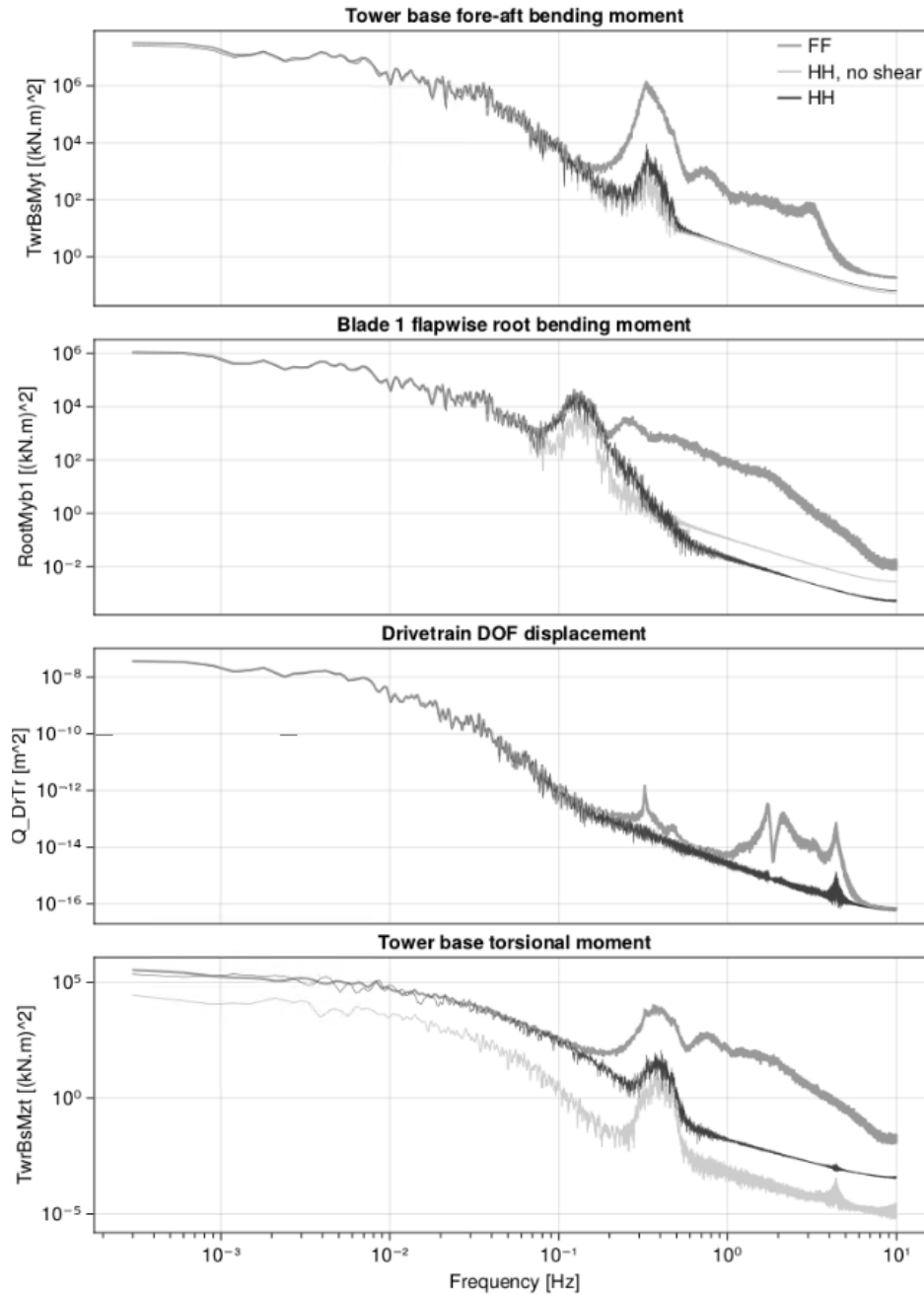


Figure 15. Various loads on single turbine with point-based (FF) and aggregated (HH) turbulence representations

4.1.3 Efficiency

FAST.Farm simulations with aggregated wind speeds show a ratio CPU time/simulated time of 0.9. As FAST.Farm is fully parallelized (it runs on multiple cores, but not yet on multiple nodes of a cluster), this means that if one disposes of one CPU core per turbine per seed, plus one core per seed for the wake dynamics, the set of simulations runs slightly faster than real time.

An effective low-hanging fruit to improve computational time lies in the way FAST.Farm reads in data from TurbSim.Farm: currently this is performed by file I/O at each timestep, while preloading wind data into memory would be much more efficient and would require only minor changes in FAST.Farm.

4.2 Use with stochastic state-space model

In the probabilistic analysis tool of D4.1 introduced in Section 2.1, SINTEF's STAS program was used to generate linear state-space models of a direct-drive DTU 10 MW wind turbine at several operating points, defined by the mean inflow wind speed, turbulence intensity and the power command⁴. An excerpt of response spectra as function of power command is shown in Figure 15, with a wind speed of 10 m/s and class B turbulence intensity (approximately 18%). From left to right and top-down: fore-aft nacelle acceleration, side-to side nacelle acceleration, flapwise blade root bending moment and pitch angle. The dark blue curve corresponds to a power command of 10 MW (full power) and orange of 0MW. Intermediate colors are 6, 4 and 2 MW.

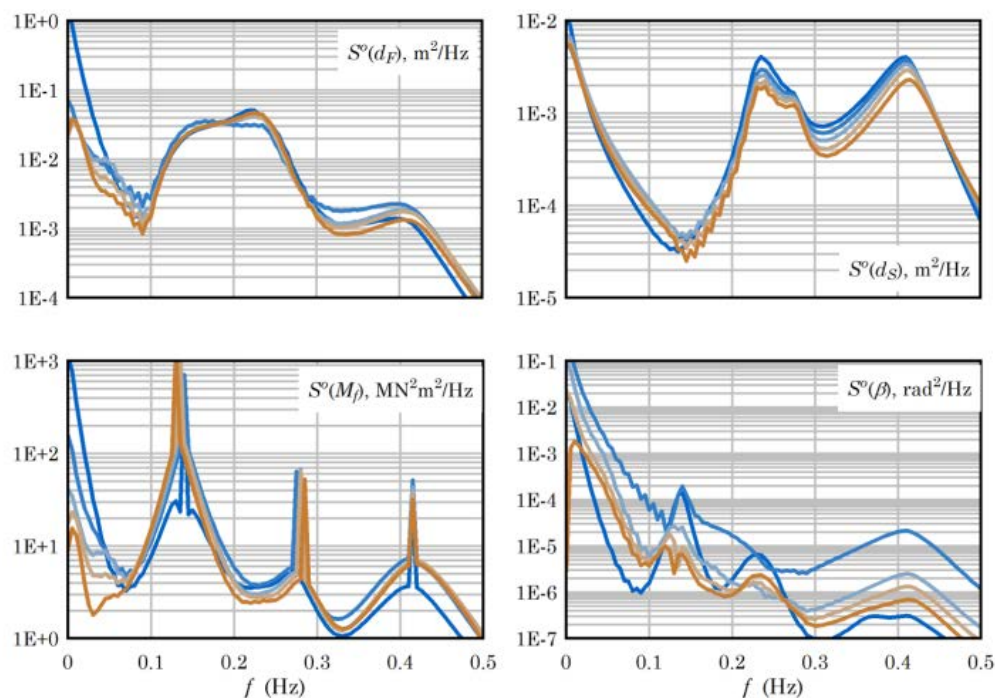


Figure 16. Trends in the output spectra with power command from D4.1 DLL

There was however no farm-level consideration, the focus being on the turbine response (structural loads) rather than on power fluctuations. Results from D4.1 and D4.2 (present report) are therefore complementary: the idea is to use the DLL during farm simulations, to get the load spectra and eventually damage rate, with the actual wind speed and turbulence intensity taking into account wake effects. To this end, the observed wind speed (i.e. rotor-averaged as reconstructed from turbine response rather than the anemometer measurement) from each turbine may be filtered to the turbine-scale time constant (typically 10 minutes) and used as input

to the DLL. An example is shown in Figure 17 where turbine 3 is in the wake of turbine 1 and a low-pass Butterworth filter of order 2 with cutoff at 10 minutes has been used. The unfiltered values are plotted in dotted lines. The turbulence intensity may partly be observed from measurements, but may also be estimated based on undisturbed wind measurements and modelled added wake turbulence.

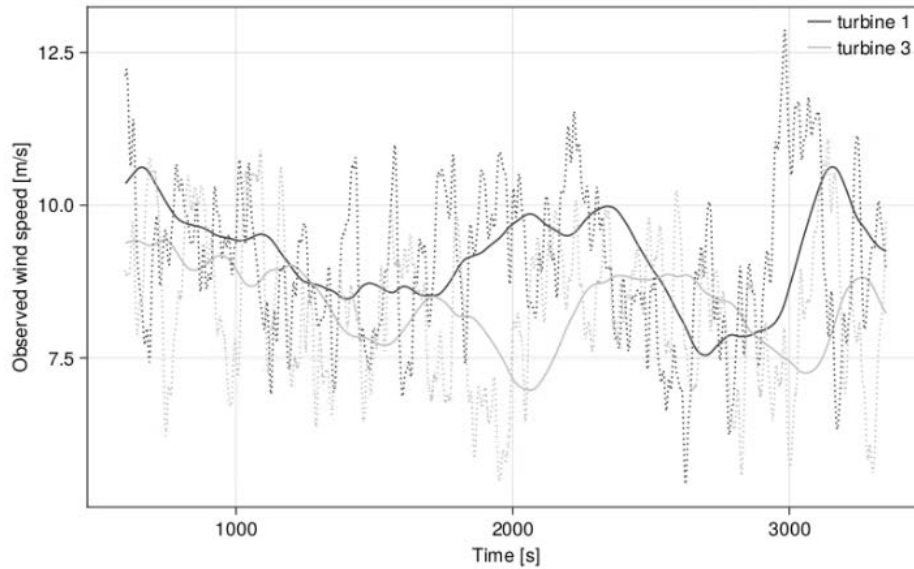


Figure 17. Timeseries of filtered observed wind speed for upwind and downwind turbines

5 CONCLUSIONS

An add-on to NREL's FAST.Farm called TurbSim.Farm was developed for efficient inclusion of farm-scale turbulence in farm simulations. The main motivation is to capture power fluctuations to be used in multi-objective hierarchical wind farm control: tracking a power command from the grid instead of maximising power offers the possibility to derate selected turbines based on their fatigue damage index. This fatigue damage may in turn lead to failures to be handled by O&M planning together with corrosion-related failures, hence closing the loop with the rest of the WATEREYE project.

TurbSim.Farm is a synthetic turbulence generator based on the concept of aggregated turbulence. It is designed for use as input to FAST.Farm but may be used as input to other farm simulators or standalone. It greatly improves accuracy and/or efficiency compared to point-based Gaussian process-based synthetic turbulence generators such as NREL's TurbSim, appropriate for turbine scale. Compared with CFD-based solution, efficiency is drastically improved but a validation study remains to be done, for instance by comparing with power fluctuations from a real wind farm in various wind conditions.

The goal of this deliverable is to provide a real-time probabilistic analysis tool. In practice, propagation of short-term (1-h) statistics to long term is made by joint use of a parameterized short-term database and a long-term joint probability distribution of the corresponding parameters. Here, this would need building a database of statistical quantities of interest from farm simulations for a set of wind speeds, directions and turbulence intensities. A power command from the grid may be added to this list, introducing derating control. Long-term analyses and derating control are covered in WATEREYE's D4.4 report.

It is the database of simulations that will be used in real time for decision making. The simulations themselves may be run offline beforehand. Still, computational efficiency to build the database and adapt to changes in wind farm or environmental properties is crucial. As seen in Sections 3.4.2 and 4.1.3, TurbSim.Farm and FAST.Farm are highly efficient and run close to real time. The storage size of the database is also of concern. TurbSim.Farm shows a drastic improvement compared with CFD-based ambient wind modelling, reducing storage size from the order of terabyte to gigabyte, greatly improving flexibility and sharability.

6 REFERENCES

- ¹ A. Næss and T. Moan, *Stochastic Dynamics of Marine Structures* (Vol. 9780521881555), Cambridge University Press. <https://doi.org/10.017/CBO9781139021364>, 2012.
- ² T. Burton, N. Jenkins, D. Sharpe and E. Bossanyi, *Wind Energy Handbook Second Edition*, Chichester, West Sussex, U.K.: John Wiley & Sons, 2011.
- ³ E. Bachynski, "Fixed and floating offshore wind turbine support structures," *Offshore Wind Energy Technology*, no. <https://doi.org/10.1002/9781119097808.ch4>, pp. 103-142, 2018.
- ⁴ K. Merz, V. Chabaud and K. Kölle, "DLL implementing a probabilistic state-space WF model," WATEREYE deliverable D4.1, 2021.
- ⁵ K. Merz, "STAS Aeroelastic 1.0 - Theory Manual," SINTEF Energy Research, 2018.
- ⁶ K. Merz, "STAS Electric 1.0 - Theory Manual," SINTEF Energy Research, 2019.
- ⁷ J. M. Jonkman, "FAST.Farm user's guide and theory manual," NREL, 2019.
- ⁸ Larsen, G. C. et al., "Dynamic wake meandering modeling," DTU Risø National Laboratory, 2007.
- ⁹ P. Sørensen, A. D. Hansen and P. A. Carvahlo Rosas, "Wind models for simulation of power fluctuations from wind farms," *Journal of wind engineering and Industrial aerodynamics*, vol. 90, pp. 1381-1402, 2002.
- ¹⁰ P. Sørensen, Cutululis, N. Antonio, A. Viguera-Rodriguez, H. Madsen, P. Pinson, L. Jensen, J. Hjerrild and M. H. Donovan, "Modelling of Power Fluctuations from Large Offshore Wind Farms," *Wind Energy*, no. 11, p. 29.43, 2008.
- ¹¹ V. Chabaud, "Synthetic turbulence modelling for offshore wind farm engineering models using coherence aggregation," *Submitted to Wind Energy*, 2023 (submitted).
- ¹² IEC, "IEC standard 61400-1 Ed. 3.0 Wind Turbines - Part 1: Design requirements," 2005.
- ¹³ A. Viguera Rodriguez, P. Sørensen, N. A. Cutululis and M. H. Donovan, "Wind model for low frequency power fluctuations in offshore wind farms," *Wind Energy*, no. 13, pp. 471-482, 2010.
- ¹⁴ J. Apt, "The spectrum of power from wind turbines," *Journal of Power Sources*, no. 169, pp. 369-374, 2007.
- ¹⁵ E. Cheynet, J. Jakobsen and J. Reuder, "Velocity Spectra and Coherence Estimates in the Marine Atmospheric Boundary Layer," *Boundary-Layer Meteorology*, p. 169:429–460, 2018.
- ¹⁶ A. Viguera-Rodriguez, P. Sørensen, A. Viedma, M. H. Donovan and E. Gómez Lázaro, "Spectral coherence model for power fluctuations in a wind farm," *Journal of Wind Energy and Industrial Aerodynamics*, no. 102, pp. 14-21, 2012.
- ¹⁷ Veers, P. S. , "Three-dimensional wind simulation", Sandia National Labs., Albuquerque, 1988
- ¹⁸ Huang, G. et al., "New Formulation of Cholesky Decomposition and Applications in Stochastic Simulation," *Probabilistic Engineering Mechanics*, no. 34, pp. 40-47, 2013.
- ¹⁹ K. B. Petersen and M. S. Pedersen, "The matrix cookbook," 2012.

²⁰ B. J. Jonkman, "TurbSim user's guide," NREL, 2016.

²¹ K. Merz, K. Kölle and A. Holdyk, "An electromechanical Model of the TotalControl Reference Wind Power Plant," SINTEF Energy Research, Trondheim, 2019.

²² M. H. Hansen and L. C. Henriksen, "Basic DTU Wind Energy Controller," DTU Wind Energy, 2013.